Experimental Study on the Application of Flat Spin to Vertical Landing of a Fixed-Wing Small UAV

Higashino, Shin-Ichiro
Department of Aeronautics and Astronautics, Kyushu University

NAKAMA, Kota
Department of Aeronautics and Astronautics, Kyushu University

SUMITOMO, Yuki
Department of Aeronautics and Astronautics, Kyushu University

出版情報：Transactions of the Japan Society for Aeronautical and Space Sciences, Aerospace Technology Japan. 20, pp.1-9, 2022. 日本航空宇宙学会
バージョン：

Trans. JSASS Aerospace Tech. Japan
Vol. 20, pp. 1-9, 2022
DOI: 10.2322/tastj.20.1

Experimental Study on the Application of Flat Spin to Vertical Landing of a Fixed-Wing Small UAV

By Shin-Ichiro HIGASHINO,[1)] Kota NAKAMA,[1),2)] and Yuki SUMITOMO[1),2)]

[1)] *Department of Aeronautics and Astronautics, Kyushu University, Fukuoka, Japan*
[2)] *Currently Kawasaki Heavy Industries, Kakamigahara, Japan*

(Received January 22nd, 2021)

The flat spin of a fixed-wing airplane is usually considered to be dangerous, and should be avoided by all means. However, an airplane in a flat spin descends almost vertically and relatively slowly. It can be used as a means of vertical landing, especially for a small fixed-wing unmanned aerial vehicle. Controlling the impact speed to the ground and touchdown position is necessary to realize the application of flat-spin landing. A large pitch-up moment generated by the combination of an all-flying tail and the gyro precession due to the yawing motion generated by the so-called P-factor of the propeller rotation was found to be effective not only for the rapid entry into flat spin, but also to control the pitch attitude and rate of descent during a flat spin. In this paper, the results regarding the relationships among the deflection angle of the all-flying tail, the rotational speed of the propeller, the spin rate, and the rate of descent obtained by flight tests using a small unmanned aerial vehicle are presented as fundamental knowledge towards the realization of practical flat-spin landing.

Key Words: Flat Spin, Vertical Landing, All-Flying Tail, Gyro Precession, Flight Tests

Nomenclature

b	:	wing span, m
C_D	:	drag coefficient
g	:	gravitational acceleration, m/s^2
m	:	mass of the UAV, kg
n	:	rotational speed of a propeller, rpm
r	:	yaw rate, deg/s
S	:	wing area, m^2
w_{EAS}	:	equivalent rate of descent, m/s
δ_e	:	elevator or all-flying tail deflection angle, deg
δ_a	:	aileron deflection angle, deg
δ_r	:	rudder deflection angle, deg
μ	:	advance ratio
θ	:	pitch angle, deg
ρ_0	:	air density at sea level in standard atmosphere, kg/m^3
ψ	:	yaw angle, deg

1. Introduction

Fixed-wing unmanned aerial vehicles (UAVs) used especially for practical missions are sometimes obliged to operate in environments where a runway or sufficient amount of flat land to enable a conventional take-off and landing are not available. A catapult[1)] is widely used as a launch method in such environments. However, there is no handy and decisive method for the recovery phase. A parachute recovery method [2)] is easy to use, but it is hard to precisely predict the UAV's touchdown point, especially when the wind is strong, and a UAV is sometimes damaged due to the impact against a rough ground surface. A net-catch method[3,4)] is also used, but it requires relatively large and heavy equipment. The authors have been keenly aware that a handy and reliable recovery method for a fixed-wing UAV operated in undeveloped environments is necessary for practical missions.

In this study, the authors focus on the spin of a fixed-wing UAV, and aim to apply it to a vertical landing method. The spin of a fixed-wing airplane is recognized as dangerous because it often results in the aircraft crashing unless correct recovery control is applied. The spin is categorized as steep spin, moderately steep spin, moderately flat spin and flat spin depending on the angle-of-attack range during the spin.[5)] Steep spin sometimes gradually develops to flat spin wherein the angle-of-attack becomes significantly larger, and it is almost impossible to recover from it applying usual recovery control input. However, there is a large increase in drag and the rate of descent is drastically reduced during a flat spin. If we can control the rate of descent and the position for the touchdown as intended, we can retrieve a fixed-wing UAV even in a narrow space using vertical descent, like the auto-rotation of a helicopter.

In order to realize a "flat-spin landing", the method for easy spin entry as intended, the controllability of both the rate of descent and the pitch-and-roll attitude of the UAV just before touchdown, and the ability to move in a horizontal direction to a desired touchdown point are essential. There are many studies[5-11)] on spin and flat spin, but all of these studies focus on understanding the characteristics,[5,6)] effective design

method for preventing spin,[7] and effective methods for recovering from spins.[7,8] There have been no studies that positively utilize the flat spin as a means of vertical landing.

In this paper, a method for entering a UAV into a flat spin intentionally and quickly, the method of controlling the pitch-and-roll attitude during a flat spin, and the method for reducing the rate of descent are the focus and examined experimentally. The fundamental results obtained by flight tests using a small UAV are shown, which will contribute to the realization of the automatic flat-spin landing.

2. Flight Test Setup

2.1. Tested UAV

The authors used a conventional small UAV named "Phoenix," as shown in Fig.1. The specifications of Phoenix are shown in Table 1. The mass of the UAV changed slightly throughout the series of multiple flight tests, mainly due to changing the mounted objects such as batteries and instruments. The differences in mass are designated as "Mass #1," "Mass #2," and "Mass #3" in later sections.

Fig.1. Tested airplane "Phoenix".

Table 1. Specifications of "Phoenix".

Items	Values
Wingspan	2.77 [m]
Wing area	0.575 [m^2]
Wing aspect ratio	12.7
Horizontal tail span	0.508 [m]
Horizontal tail area	0.070 [m^2]
Horizontal tail aspect ratio	3.69
Ratio between area of elevator and horizontal tail	0.257
Length	1.50 [m]
Mass	Mass #1 : 7.49 [kg] Mass #2 : 8.10 [kg] Mass #3 : 8.17 [kg]
C.G. position	28.0 [%] MAC
Stick-fixed neutral point h_n	47.4 [%] MAC
Propulsion motor	Hacker A50-12L
Propeller(folding)	14×10 [in] (35.56×25.4[cm])

Phoenix was originally designed as a motor-glider UAV and combined with a rubber balloon for aerosol observation and recovery missions from a high altitude.[2] Therefore, it was not designed especially for aerobatic maneuvers including flat spins. It has ample payload space in the mid-fuselage under the canopy, as shown in Fig.1.

It is widely known that shifting the center-of-gravity (C.G.) position toward the rear of the aircraft tends to make the airplane spin easier.[6,9] However, as the method for spin development in this study does not rely on shifting the C.G. position, the C.G. was not changed for any of the flights. It was kept constant throughout all flight tests as 28% of the mean aerodynamic chord (MAC) length, while the stick-fixed neutral point (N.P.) is 47.4% of MAC.

The only point to change from the original configuration was the use of an all-flying tail (AFT), as shown in Fig.2 instead of the original tail; that is, a conventional combination of a horizontal stabilizer and an elevator, as shown in Fig.3. The wing areas of the two are the same. An AFT is reported to be effective for pitch control at the time of a deep stall.[10,11] The deflection angle of the AFT can be changed over a wide range, as shown in Fig.2 (b), in order to generate large pitch-up moment even at a large angle-of-attack. The specifications of the original tail and the AFT are summarized in Table 2.

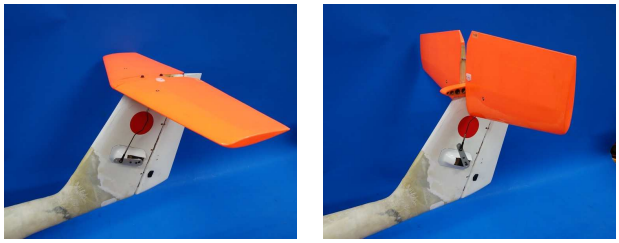

(a) $\delta_e = 0$ deg (b) $\delta_e = -90$ deg

Fig.2. AFT of Phoenix.

(a) $\delta_e = 0$ deg (b) $\delta_e = -25$ deg

Fig.3. Original horizontal tail of Phoenix.

Table 2. Specifications of the original tail and the AFT.

Items	Original tail	AFT
Span	0.508 [m]	0.508 [m]
Area	0.070 [m^2]	0.070 [m^2]
Aspect ratio	3.69	3.69
Area ratio (elevator / stabilizer)	0.257	1.00
Deflection angle ragne	-30〜+30 [deg]	-100〜+20 [deg]

2.2. Instrumentation

A schematic of the data acquisition and control system of the UAV is shown in Fig.4. Two GPS-aided inertial navigation sensors (GPS/INS) 3DM-GX5-45(Manufacturer: LOAD) and MTi-G (Manufacturer: XSENS) were installed for measurement. Fundamental motion data such as Euler angles, 3-axis angular rates and accelerations, and the GPS position were obtained using the 3DM-GX5-45. The specifications of the major sensors equipped in the 3DM-GX5-45 are shown in Table 3. Since MTi-G was used only for examining the directional control capability,[12] the specifications are not shown here. 3DM-GX5-45 is also equipped with an absolute pressure sensor, and its output was used to calculate the rate of descent during a flat spin by differentiating the pressure altitude because it has both a higher accuracy and higher sampling rate than those of GPS output. The propeller rotational speed was measured using a Hall sensor and a tiny magnet attached to the motor shaft.

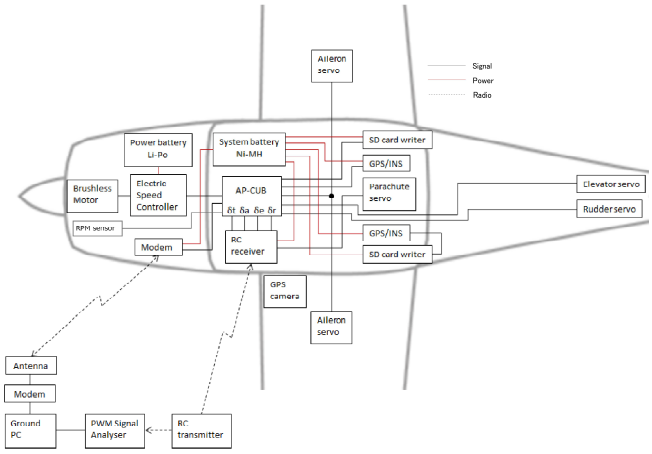

Fig.4. Schematic of the data acquisition and control system.

Flight control except for the flat spin was basically conducted through manual operation. However, the flat spin was conducted using an in-house FCC named "AP-CUB",[13] which was originally developed as a multi-purpose FCC for a UAV. The reason for using the FCC is to maintain the repeatability of the operation and to avoid crashing due to the possibility of an error occurring in complicated manual control during a flat spin. The data was recorded onto an onboard micro SD card, and was simultaneously monitored at a ground station via a wireless communication link.

An emergency parachute recovery system with an ejection-type pilot parachute was developed, as shown in Fig.5. It was flight tested and equipped just in case of an unexpected failure or phenomena during the flight tests. This system is different from a general "spin recovery parachute system",[14] which is usually installed in the tail section. This system was designed to deploy the main parachute following the ejection of the pilot parachute from the top of the canopy even if the parachute hatch on top of the fuselage is in the wake of the fuselage during a flat spin. Once it is activated, the UAV cannot land in the conventional way, and has to be recovered using the main parachute.

Table 3. Specifications of LORD 3DM-GX5-45.

Inertial Measurement Unit (IMU)		
	Accelerometer	Gyroscope
Range	±8 [G]	300 [deg/s]
Non-linearity	±0.02 [%FS]	±0.02 [%FS]
Bias instability	±0.04 [mG]	8 [deg/hr]
Scale factor stability	0.03 [%]	±0.05 [%]
Resolution	0.02 [mG]	<0.003 [deg/s]
Sampling rate	1 kHz	4 kHz
Pressure Altimeter		
Altitude range	260-1260 [hPa]	
Resolution	0.01 [hPa] RMS	
Relative accuracy	±0.1 [hPa] (800-1000 [hPa]@25 [℃])	
Sampling rate	25 [Hz]	
Computed Output		
Position accuracy	±2 [m] RMS horizontal, ±5 [m] RMS vertical	
Velocity accuracy	±0.1 [m/s] RMS	
Attitude accuracy	EKF outputs: ±0.25[deg] RMS roll and pitch, ±0.8[deg] RMS heading (typ) CF outputs: ±0.5[deg] roll, pitch, and heading (static, typ), ±2.0[deg] roll, pitch, and heading (dynamic, typ)	
Attitude resolution	< 0.01[deg]	
Calculation update rate	500 [Hz]	
GNSS Output		
Receiver type	72-channel GPS/QZSS L1 C/A, SBAS L1 C/A:WAAS, MSAS	
Output rate	1 [Hz] to 4 [Hz]	
Horizontal position accuracy	GNSS 2.5 [m] SEP, SBAS 2.0 [m] SEP	

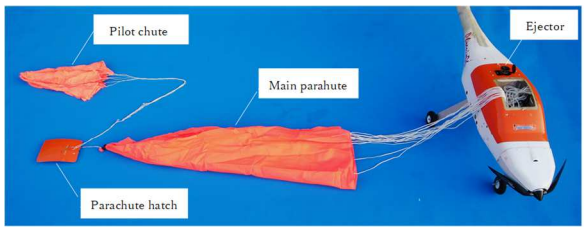

Fig.5. Emergency parachute recovery system.

3. Flight Test Method

Generally, once an airplane enters into a spin, the initial steep spin sometimes develops into a flat spin over some period of time depending on the C.G. position and characteristics of the airplane. However, an efficient method for entering any UAV into a flat spin as intended, it is necessary to conduct a flat-spin landing without waiting for the spin to develop. At the same time, an easy and appropriate recovery method from a flat spin as intended, it is also important to continue multiple flat-spin

tests during a single flight in the development phase until a reliable flat-spin landing method is established. The method that relies on shifting the C.G. position was not used in this study, as mentioned earlier. This is because that method requires a relatively bulky system for moving an object with sufficient mass in the fuselage, which is neither handy nor practical. Therefore, we used an AFT to produce large pitch-up moment during the spin.

In the flight tests, the UAV took off from a runway and climbed to a maximum altitude of approximately 300 to 400 m above the ground under manual control using a radio-control transmitter. All of the tests were conducted under the permission of the Japan Civil Aviation Bureau (JCAB) because the maximum altitude reached beyond the limit below UAVs can fly without permission (i.e. 150m above ground level). After reaching the maximum altitude, the pilot stopped the propeller rotation, and gradually pulled the elevator stick of the radio-control transmitter while simultaneously applying full left rudder. The direction of rudder deflection had something to do with the propeller rotational direction in this study, and it was therefore maintained to full left. The reason is explained in detail later. After the UAV stalled and dropped the left wing and nose, the pilot switched control from manual to automatic. All the pilot had to do was put the UAV into a spin following the usual procedure for doing it and then switch to automatic control. After control was switched to the FCC, full throttle, a preset deflection angle of the AFT, and full left rudder were applied automatically, and the UAV quickly and easily entered into a flat spin. After the UAV lost altitude approximately 100 to 150m in the flat spin, the pilot once again switched back to manual control. By putting all control stick positions back to neutral and moving the throttle to idle, the spin rotation stopped and the UAV entered a vertical dive. The pilot gradually pulled the nose up and then repeatedly conducted the test over again by climbing to the maximum altitude and starting the process over again. This was done as long as the battery lasted. Two to three flat-spin tests were usually conducted in one flight. After the test maneuvers were completed, the UAV landed on a runway in a usual manner under manual control. One flight was completed in approximately 5-6 min.

4. Flight Test Results and Discussion

4.1. Intentional entry into flat spin using the AFT

In order to confirm the effectiveness of the AFT, two flight test results are compared here. Figure 6 (a) shows the spin data using the original tail, and Fig.6 (b) shows the spin data using the AFT. The figures include the elevator deflection angle δ_e, the rate of descent w_{EAS} (designated as w in Figure 6), the yaw rate r, the pitch angle θ, and the heading angle ψ, respectively. The rate of descent w_{EAS} in equivalent airspeed was calculated by differentiating the pressure altitude, which was corrected for non-standard air temperature, and static pressure measured on the ground.

For the test shown in Fig.6 (a), the elevator deflection angle δ_e of the original tail was kept maximum to its full-up position (-25 deg) during the spin. The rudder was deflected maximum to the left (18 deg), the aileron was kept neutral, and the propulsion motor was shut off. As seen from Fig.6 (a), pitch angle θ dropped to almost -70 to -80 deg, the yaw rate r stayed negative during the spin, and the heading angle ψ decreased continuously; that is, aircraft spun counterclockwise as viewed

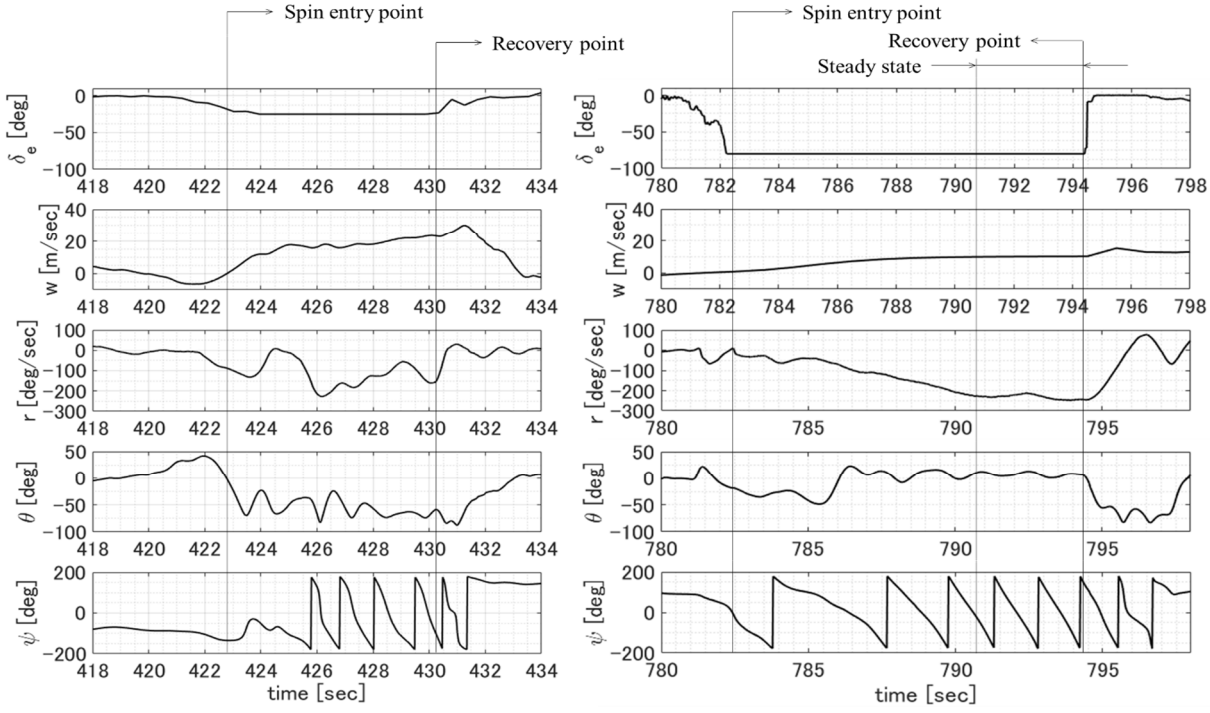

Fig.6. Flight data during (a) a steep spin using a conventional tail and (b) a flat spin using an AFT at full throttle.

from above, and this is considered to be a typical steep spin. The rate of descent w_{EAS} increased gradually up to approximately 20 to 25 m/s, which is slightly less than the typical flight speed in level flight.

In the test shown in Fig.6 (b), the AFT was deflected as -80 deg and full throttle (propeller rotational speed: 9200 rpm) was applied. The deflection angles of the aileron δ_a and rudder δ_r were the same as in the test shown in Fig.6 (a). It is obvious looking at Fig.6 (b) that the pitch angle decreased once to around -30 to -50 deg just after the AFT was deflected as -80 deg, and then it increased to almost zero or even positive values during the spin. The heading angle ψ decreased continuously in the same direction; that is, the aircraft spun counterclockwise as viewed from above, obviously signifying a flat spin. The rate of descent w_{EAS} increased to at most approximately 10 m/sec, and this was much less than that shown in Fig.6 (a). The yaw rate r remained negative during the spin and gradually increased in magnitude. Its fluctuation was much smaller than that shown in Fig.6 (a). The rate of descent w_{EAS}, yaw rate r, and pitch angle θ for the duration, designated as "Steady-state" at the top of Fig. 6(b) were and plotted in the graphs in the following sections. From Fig.6, the AFT was found to be very effective for quickly realizing a flat spin and slowing the rate of descent. The effect of propeller rotational speed to pitch attitude was also found by coincidence during the series of flight tests, and its effect as well as the effect of the AFT deflection angle are discussed in later sections. It should be noted that the flight path during the flat spin using this method has been partially published in other literature.[12)]

4.2. Effect of AFT deflection angle on flat spin

In this section, flight test results of 24 spin maneuvers are shown for investigating the effect of AFT deflection angle on the pitch attitude and the rate of descent in a flat spin. In the flight tests, motion data were obtained by maintaining AFT deflection angle to a certain constant value that results in a steady spin. The duration for the steady part of one spin maneuver was approximately 5 to 10 s depending on the rate of descent. The angles of the control surfaces and the throttle position during the spin were kept constant using the FCC, as shown in Table 4. Note that the effect of propeller rotational speed is included in the results in this section because full throttle was applied throughout all of the tests in this section. The effect of the propeller rotational speed is separately evaluated in the next section.

Table 4. Values of the control surface deflection angles and throttle position.

Items	Values
Throttle position	100 [%](8652 rpm)
Aileron	0 [deg]
Rudder	18 [deg]
AFT	a certain constant value from -100 to -39 [deg]

Figure 7 shows the relationship between the deflection angle of the AFT δ_e and mean pitch angle θ with standard deviations. During the series of tests, the mass of the UAV changed slightly as mentioned before, and the difference in mass is expressed as the difference in color of the data points in the figure. An error bar at each data point indicates the standard deviation during the period of each steady spin. It is obviously seen that the pitch angle θ clearly increased to the positive direction as the AFT deflection angle δ_e increased in absolute magnitude. An effect of difference in mass is not clearly seen. The pitch attitude became almost zero when the AFT deflection angle δ_e was around -70 deg, and this pitch attitude is quite suitable for landing on the ground. The pitch angle increased, even for positive values, and it reached a maximum of over 10 deg when δ_e= -90 deg, then decreased when δ_e was deflected -100 deg. This means the AFT probably stalled at around δ_e= -100 deg. It should be noted that roll angle was always stable around 0 deg in all spin maneuvers.

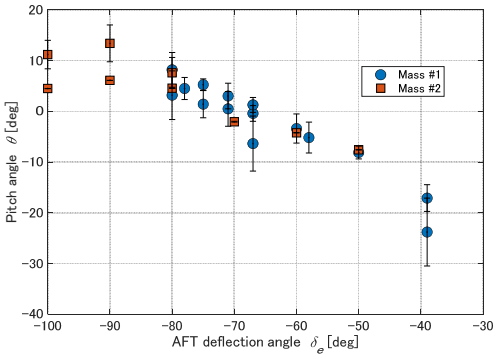

Fig.7. Relationship between AFT deflection angle δ_e and pitch angle θ.

In order to examine the operating state of the AFT, flow visualization of the AFT using tufts was conducted during flights. Two separate micro cameras were installed in a camera holder at the tip of the tail boom, as shown in Fig.8. Pictures of the lower surface (suction side) of the AFT during the spin with δ_e= -100, -90, and -80 deg are shown in Fig.9. The vertical positions and colors of the right and left side of the AFT in Fig.9 are slightly different due to the difference in the installation angle of the two micro cameras. As can be seen from Fig.9(a),

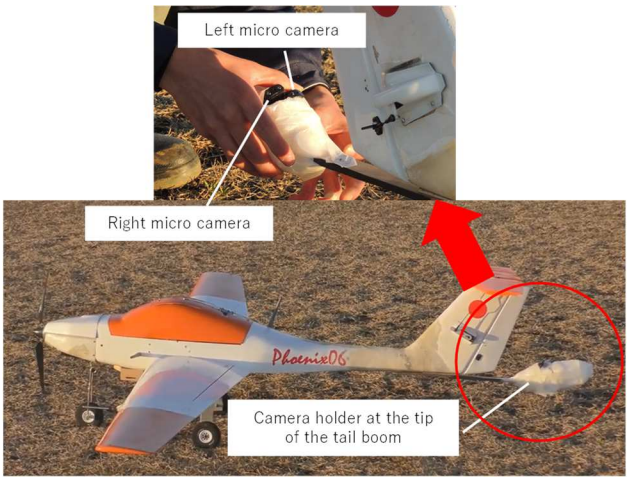

Fig.8. Two micro cameras installed in the camera holder at the tip of the tail boom

(a) δ_e= -100 [deg]

(b) δ_e= -90 [deg]

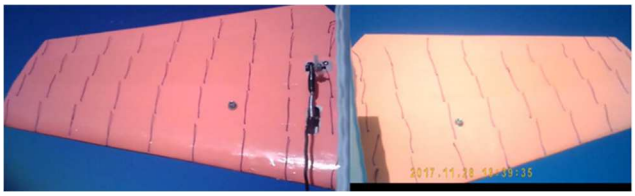

(c) δ_e= -80 [deg].

Fig.9. Results of flow visualization on the lower side of the AFT during spins with (a) δ_e= -100 [deg], (b) δ_e= -90 [deg], and (c) δ_e= -80 [deg].

the tufts are disturbed when δ_e= -100 deg, and the flow looks separated from the surface. However, no separation is found when δ_e= -90 deg and δ_e= -80 deg (Fig.9(b) and Fig.9(c), respectively). These pictures indicates that the effect of the propeller slipstream is considered relatively small because the stall angle-of-attack of the AFT is within the angles between δ_e= -90 deg and δ_e= -100 deg, which implies that the direction of the resultant airflow vector to the AFT is close to the direction of the relative airflow vector due to the vertical descent.

Next, the relationship between the AFT deflection angle δ_e and the yaw rate r is shown in Fig.10. The relationship between the two is not so clear, but it looks the yaw rate r has a tendency to increase in absolute magnitude; that is, spin rotation speed increases as the absolute magnitude of δ_e increases. It is also seen that the mean yaw rate r of multiple data points in the case of a larger mass (Mass #2, red squares) is lower, in general, in absolute magnitude than that of the case of smaller mass (Mass #1, blue circles); that is, the smaller the mass, the faster the spin rotation.

Figure 11 shows the relationship between the AFT deflection angle δ_e and the rate of descent w_{EAS}. It is seen that the rate of descent w_{EAS} decreased gradually as δ_e increased in absolute magnitude. The minimum rate of descent reached was approximately 7 m/s. It is clearly seen that the difference in mass results in a distinctive difference in the rate of descent; that is, the smaller the mass, the slower the rate of descent.

From these figures, it can be said that increasing the AFT deflection angle in absolute magnitude is quite effective for flattening the pitch attitude during the spin and decreasing the rate of descent, which will be very important for the moment of impact on the ground. The rate of descent is easily affected by the difference in mass, while it is hard to have an effect on pitch attitude. The effect of mass will be discussed at the end of the next section.

Non-dimentional advance ratio μ is often used as a parameter for expressing the operating state of a rotating wing such as a propeller and helicopter blades.[15] Since the flat spin of a fixed-wing airplane is similar to the autorotation of a helicopter, the results are evaluated in non-dimentional form here using the advance ratio μ and drag coefficient C_D. Note that the advance ratio μ is not the advance ratio of the propeller, but the advance ratio of the UAV itself in a flat spin. In this study, the advance ratio μ and drag coefficient C_D are defined as Eq.(1) and Eq.(2), respectively.

$$\mu = \frac{w_{EAS}}{|r|(b/2)} \tag{1}$$

$$C_D = \frac{2mg}{\rho_0 {w_{EAS}}^2 S} \tag{2}$$

For the calculation of drag coefficient, the projected area of the UAV including fuselage and tail to the horizontal plane may be taken as the reference area, but the wing area was utilized in this study for simplicity

The relationship between the advance ratio μ of the UAV and drag coefficient C_D is shown in Fig.12. It is seen from the figure that the drag coefficient C_D clearly increased as

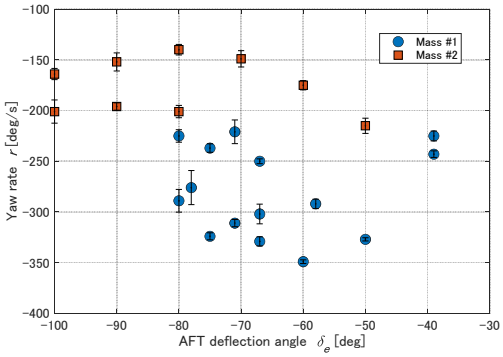

Fig.10. Relationship between AFT deflection angle δ_e and yaw rate r.

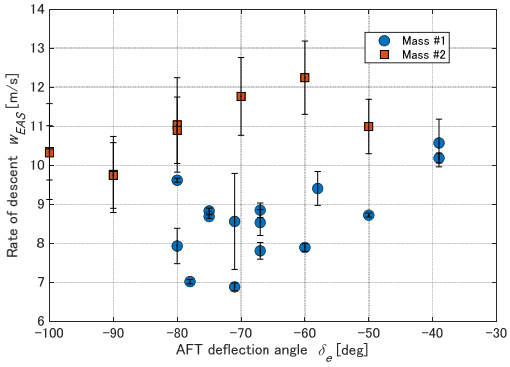

Fig.11. Relationship between AFT deflection angle δ_e and the rate of descent w_{EAS}.

the advance ratio μ decreased. In order to increase the drag coefficient and reduce the rate of descent, decreasing the advance ratio by increasing the yaw rate will be effective.

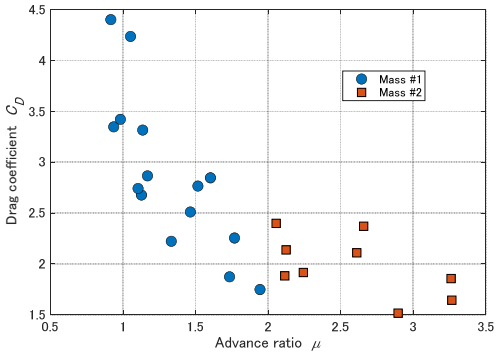

Fig.12. Relationship between the advance ratio μ and drag coefficient C_D for varying the AFT deflection angle.

4.3. Effect of propeller rotational speed on flat spin

The effect of the propeller rotational speed on the pitch angle θ, yaw rate r, and the rate of descent w_{EAS} was also examined by changing the rotational speed of the propeller per one spin for eight spins. The positions of the control surfaces other than the throttle was kept constant, as shown in Table 5. The throttle settings of 0, 25, 50, 75, and 100 % correspond to the average propeller rotational speed of 0, 3198, 5580, 7477, and 8652 rpm, respectively. It should be noted that the results when the propeller rotational speed was $n = 0$ expresses the effect of the AFT only. In the series tests examining the effect of the propeller rotational speed, the mass of the UAV was 8.1 kg (Mass #3 in Table 1).

Table 5. Values of the control surface deflection angles and throttle position.

Items	Values
Throttle position	A certain constant value from 0 to 100 [%]
Aileron	0 [deg]
Rudder	18 [deg]
AFT	-80 [deg]

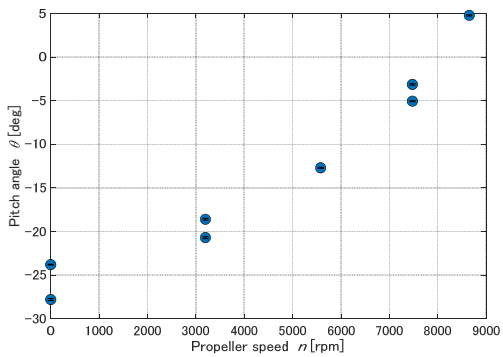

Fig.13. Relationship between the propeller rotational speed n and pitch angle θ.

Figure 13 shows the relationship between the propeller rotational speed n and mean pitch angle θ. It is clearly seen that the pitch angle θ increased, even to positive values, as the propeller rotational speed n increased. This effect is considered as the gyro precession of the propeller rotation caused by the yawing moment due to the so-called "P-factor," which is caused by a large angle-of-attack during a flat spin. Uneven thrust on the right- and left-hand sides of the propeller rotational plane due to the large angle-of-attack generated the yawing moment (P-factor), and this yawing moment acted as the external torque to the rotating propeller. The resulting gyro precession torque acted as the pitch-up moment, as illustrated in Fig.14. Therefore, the pitch-up moment is effectively generated only when the spin direction is counterclockwise, in our case when viewed from above, because the rotational direction of the propeller is counterclockwise when viewed from the front.

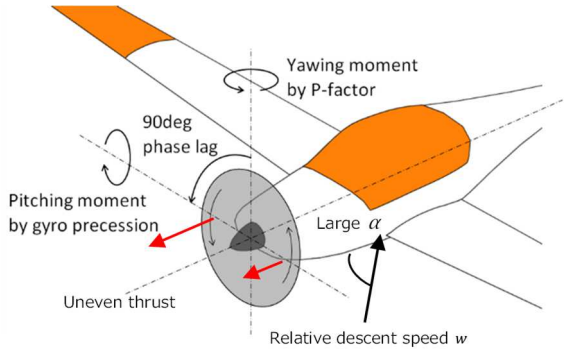

Fig.14. P-factor and gyro precession.

The relationship between the propeller rotational speed n and the yaw rate r is shown in Fig.15, and the relationship between the propeller rotational speed n and the rate of descent w_{EAS} is shown in Fig.16. It is seen from both figures that the yaw rate r increased in magnitude and the rate of descent w_{EAS} decreased in magnitude as the propeller rotational speed n increased; that is, the faster the propeller rotational speed, the faster the spin rate and the slower the rate of descent. However, the rate of descent w_{EAS} does not change

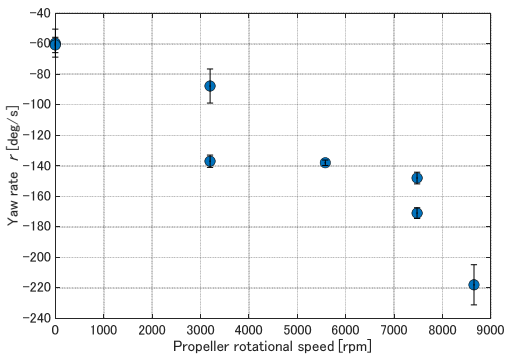

Fig.15. Relationship between the propeller rotational speed n and yaw rate r.

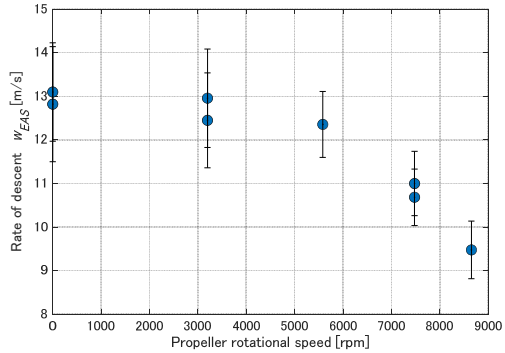

Fig.16. Relationship between the propeller rotational speed n and the rate of descent w_{EAS}.

very much when the propeller rotational speed n becomes less than approximately 5000 rpm.

Based on this data, it can be said that the tendencies of pitch attitude, yaw rate, and the rate of descent when the propeller rotational speed is increased is similar to those when the AFT deflection angle is increased in magnitude. Therefore, the combination of high AFT deflection angle and high propeller rotational speed is quite effective and suitable for landing using a flat spin.

Similar to Fig.12, the relationship between the advance ratio μ and drag coefficient C_D for varying the propeller rotational speed is shown in Fig.17. Similar to the results shown in Fig.12, the drag coefficient clearly increased as the advance ratio decreased. The relationship between the two is summarized in Fig.18 by combining Fig.12 and Fig.17. The relationship looks almost unchanged, independent of the difference in mass and the devices used to increase the pitch-up moment; that is, AFT deflection angle and propeller rotational speed. The maximum drag coefficient is reached approximately C_D=4.4.

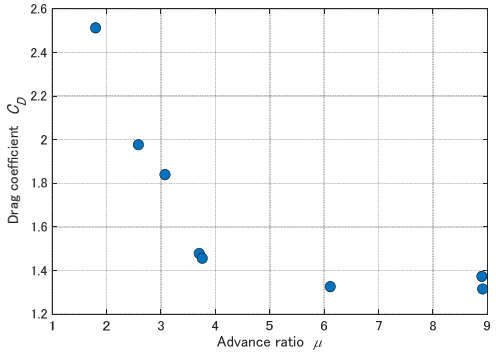

Fig.17. Relationship between the advance ratio μ and drag coefficient C_D for varying the propeller rotational speed.

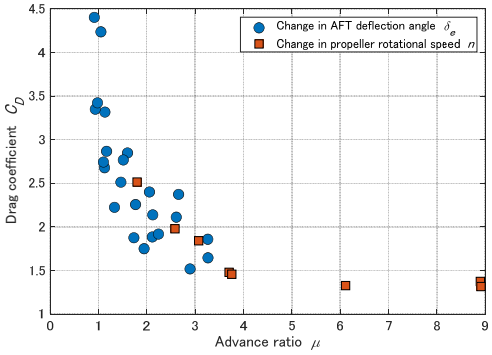

Fig.18. Relationship between the advance ratio μ and drag coefficient C_D for all data.

The rate of descent w_{EAS} can be predicted using Eq.(3) by solving Eq.(2) for w_{EAS}, and it becomes a function of wing loading mg/S.

$$w_{EAS} = \sqrt{\frac{2}{\rho C_D}\frac{mg}{S}} \tag{3}$$

The predicted w_{EAS} is shown in Fig.19 as a blue solid line by assuming the maximum drag coefficient C_D=4.4. All of the rates of descent shown in the previous figures are also shown for all mass cases. From our experience with a parachute landings,[2] a safe touchdown speed that does not damage the airframe structure of similar wing-loaded airplanes when landing on soft ground or in a grass field is less than 5 to 6 m/s. It is seen from Fig.19 that the minimum rate of descent achieved was slightly less than 7 m/s, and reducing the rate of descent further is desirable for a safe landing, although the actual touchdown speed may be reduced to some extent due to the ground effect just before touchdown.

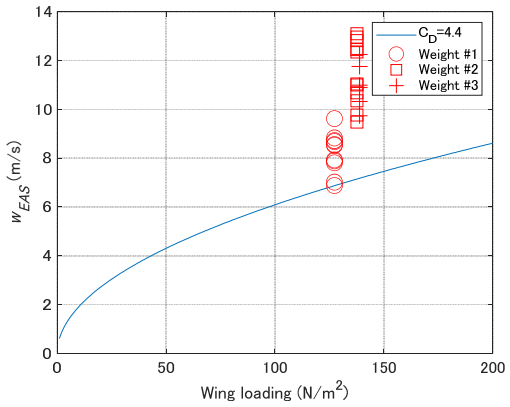

Fig.19. Comparison of the rate of descent realized and the predicted rate of descent assuming C_D=4.4.

5. Conclusion

In order to apply a flat spin in the vertical landing method of a fixed-wing UAV in a narrow space, a method for entering the UAV into a flat spin intentionally and quickly, a method for controlling the pitch attitude during a flat spin, and a method for controlling the rate of descent during a flat spin were examined experimentally.

The use of an all-flying tail (AFT) was found to be effective for entering the UAV into a flat spin intentionally and quickly, as well as for controlling the pitch attitude and the rate of descent during a flat spin. The effect of the AFT was examined

by changing the angle of the AFT, and the results showed that the pitch attitude can even become positive and the rate of descent becomes slower as the AFT deflection angle increases in absolute magnitude. The effect of the propeller rotational speed was also examined, and similar results were obtained in which the pitch attitude increased, even to the point of becoming positive, and the rate of descent decreased as the propeller rotational speed became larger. The mean drag coefficient during the spins showed a clear correlation to the advance ratio of the UAV when considering it as a rotational object independent of the difference in mass and the devices used; that is, AFT deflection angle and propeller rotational speed, with the maximum drag coefficient reaching approximately C_D=4.4. The rate of descent expressed as a function of wing loading assuming C_D=4.4 showed that a safe rate of descent of approximately 5 to 6 m/s can be obtained by reducing the wing loading.

Acknowledgments

This study was supported by JSPS KAKENHI Grant Number JP26630445 and JP20H02356.

References

1) Insitu : “Ground Support”, https://www.insitu.com/products (accessed January 5th, 2021)
2) Higashino, S., Hayashi, M., Nagasaki, N., Umemoto, and S., Nishimura, M.: A Balloon-Assisted Gliding UAV for Aerosol Observation in Antarctica, *Trans. JSASS, Aerospace Tech. Japan*, **12**, APISAT-2013(2014), pp.a35-a41.
3) Kim, H.J., Kim, M., Lim, H., Park, C., Yoon, S., Lee, D., Choi, H., Oh, G., Park, J., and Kim, Y.: Fully Autonomous Vision-Based Net-Recovery Landing System for a Fixed-Wing UAV, *IEEE/ASME Trans. Mechatronics*, **18**(2013), pp. 1320-1333.
4) Imgur : “Drone Catcher in Afghanistan”, http://i.imgur.com/AzvsTCH.jpg (accessed November 20th, 2020)
5) Burk, S. M., Jr., Bowman, J. S., Jr. and White, W. L.: Spin-Tunnel Investigation of the Spinning Characteristics of Typical Single-Engine General Aviation Airplane Designs, NASA Technical Paper 1009, 1977.
6) Klinar, W. J. and Wilson, J. H. : Spin-Tunnel Investigation of the Effects of Mass and Dimensional Variations on the Spinning Characteristics of a Low-Wing Single-Vertical-Tail Model Typical of Personal-Owner Airplanes, NACA Technical Note 2352, 1951.
7) Stough, H. P. III, Patton, J. M., Jr., Sliwa S. M. : Flight Investigation of the Effect of Tail Configuration on Stall, Spin, and Recovery Characteristics of a Low-wing General Aviation Research Airplane, NASA Technical Paper 2644, 1987.
8) Raghavendra, P. K. , Sahai, T., Kumar, P. A., Chauhan, M., and Ananthkrishnan, N., : Aircraft Spin Recovery, with and without Thrust Vectoring, Using Nonlinear Dynamic Inversion, *J. Aircraft,* **42** (2005), pp.1492-1503.
9) Bowman, J. S., Jr. : Summary of Spin Technology as Related to Light General Aviation Airplanes, NASA Technical Note D-6575, 1971.
10) Sim, A.G. : Flight Characteristics of a Manned, Low-Speed, Controlled Deep Stall Vehicle, NASA Technical Memorandum 86041, 1984.
11) Taniguchi, H. : Anlysis of Deepstall Landing for UAV, 26th International Congress of Aeronautical Sciences, Anchorage, USA, ICAS2008 5.6.4, 2008.
12) Miyazono, K., Nakama, K., Sumitomo, Y., and Higashino. S. : Study on a Fixed Point Vertical Landing Method Using the Flat Spin for a Fixed-wing UAV, *JSASS Aerospace Technology*, **19**(2020), pp.131-140.(in Japanese)
13) Higashino, S.: Development of an UAV Flight Control Module for the Operation in Antarctica, *The 5th Asian-Pacific Conference on Aerospace Technology and Science*, Guilin, China, 2006.10.,2006.
14) Bradshw, C. F. : A Spin Recovery Parachute System for Light General-Aviation Airplanes, NASA Technical Memorandum 80237, 1980.
15) Prouty, R.W. : *Helicopter Performance, Stability and Control*, Krieger Publishing Company, Melbourne (USA), 2005, p.122.